

The Influenza A Virus M2 Channel: A Molecular Modeling and Simulation Study

M. S. P. Sansom,¹ I. D. Kerr, G. R. Smith, and H. S. Son

Laboratory of Molecular Biophysics, The Rex Richards Building, University of Oxford, South Parks Road, Oxford OX1 3QU, United Kingdom

Received January 3, 1997; returned to author for revision February 27, 1997; accepted April 9, 1997

The M2 protein of influenza virus forms ion channels activated by low pH which are proton permeable and play a key role in the life cycle of the virus. M2 is a 97-residue integral membrane protein containing a single transmembrane (TM) helix. M2 is present as disulfide-linked homotetramers. The TM domain of M2 has been modeled as a bundle of four parallel M2 helices. The helix bundle forms a left-handed supercoil surrounding a central pore. Residue H37 has been implicated in the mechanism of low-pH activation of the channel. Models generated with H37 in a fully deprotonated state exhibit a pore occluded by a ring of H37 side chains oriented toward the lumen of the pore. Models with H37 in a fully protonated state no longer exhibit such occlusion of the pore, as the H37 side chains adopt a more interfacial location. Extended molecular dynamics simulations with water molecules within and at the mouths of the pores support this distinction between the H37-deprotonated and H37-protonated models. These simulations suggest that only in the H37-protonated model is there a continuous column of water extending the entire length of the central pore. A mechanism for activation of M2 by low pH is presented in which the H37-deprotonated model corresponds to the "closed" form of the channel, while the H37-protonated model corresponds to the "open" form. A switch from the closed to the open form of the channel occurs if H37 is protonated midway through a simulation. The open channel is suggested to contain a wire of H-bonded water molecules which enables proton permeability. © 1997 Academic Press

INTRODUCTION

The M2 protein from influenza A virus is a small (97-residue) integral membrane protein (Lamb *et al.*, 1985) which forms low-pH activated and proton-permeable ion channels (Pinto *et al.*, 1992; Chizhmakov *et al.*, 1996; Shimbo *et al.*, 1996). M2 is a minor component of virions, but is abundantly expressed on the plasma membrane of infected cells. M2 is composed of three domains: (a) a short (ca. 25-residue) extracellular N-terminal domain, (b) a single transmembrane (TM) domain, and (c) a longer (ca. 55-residue) intracellular C-terminal domain. The protein forms homotetramers which are stabilized by disulfide bridges formed by cysteine residues immediately N-terminal to the TM domain (Holsinger and Lamb, 1991; Sugrue and Hay, 1991; Panayotov and Schlesinger, 1992). The tetramer is either formed by a pair of disulfide-linked dimers or by a disulfide-linked tetramer. Thus, the intact protein contains a bundle of four approximately parallel TM helices packed together in close proximity to one another within the membrane.

M2 functions as an ion channel which is activated by low pH and which endows proton permeability on membranes containing it. Direct evidence for the channel function of M2 has been obtained from a number of electrophysiological studies, including heterologous expression of M2 in *Xenopus* oocytes (Pinto *et al.*, 1992), in mammalian cells (Wang *et al.*, 1994; Chizhmakov *et al.*,

1996), and in yeast (Kurtz *et al.*, 1995), and also via reconstitution of M2 protein into planar lipid bilayers (Tosteson *et al.*, 1994) and lipid vesicles (Schroeder *et al.*, 1994). M2 may play roles in both an early and a late stage of the infection cycle of influenza A. In the early stage the role of M2 appears to be to enable acidification of the interior of endocytosed virions, thus promoting release of ribonucleoprotein from the membrane (matrix) M1 protein (Helenius, 1992). M2 may also function in some strains of influenza, e.g., FPV, to modulate the pH in the *trans*-Golgi vesicles during later stages of the infection cycle, thus maintaining a high intravesicular pH which in turn prevents premature activation of hemagglutinin via a low-pH-induced conformational change (Ciampor *et al.*, 1992). The ion channel activity of M2 is blocked by the anti-influenza drug amantadine (Hay *et al.*, 1985; Chizhmakov *et al.*, 1996). This action is thought to be the basis of the therapeutic effects of amantadine, as the drug is inactive against influenza B, which lacks the M2 protein.

Low-pH activation of M2 is the key to its biological function. Detailed electrophysiological studies have revealed that activation of the channel is associated with an apparent pK_A of ca. 7 (Chizhmakov *et al.*, 1996). Examination of the sequence of M2 reveals a conserved histidine (H37) residue within the TM sequence which is a plausible candidate for the side chain associated with this pK_A . Mutation of H37 leads to M2 channels which are no longer activated by low pH (Wang *et al.*, 1995). Thus, it would seem that protonation of H37 is associated with M2 channel activation. A simple model of such acti-

¹ To whom correspondence and reprint requests should be addressed. Fax: +44-1865-510454. E-mail: mark@biop.ox.ac.uk.

vation would consist of the channel existing in two forms: a "closed" form in which H37 is unprotonated and an "open" form in which H37 is protonated.

A number of studies have probed the relationship between M2 channel function and the structure of the protein using both naturally occurring and site-directed mutants (Holsinger *et al.*, 1994). Mutations which perturb channel functions, including block by amantadine, map onto one face of the putative TM helix. This suggests that the ion channel activity of M2 is associated with the tetrameric bundle of TM helices which spans the membrane. This interpretation receives support from the observation that a synthetic peptide corresponding to the TM segment of M2 adopts an α -helical conformation in the presence of lipids (Duff *et al.*, 1992) and will spontaneously form ion channels in planar lipid bilayers (Duff and Ashley, 1992). Ion channels formed by bundles of parallel TM helices are well documented in a number of other systems, including many channel-forming peptides (Sansom, 1991, 1993), simple integral membrane proteins such as phospholamban (Arkin *et al.*, 1995), and more complex channel proteins such as the nicotinic acetylcholine receptor (Unwin, 1995; Sankaramakrishnan *et al.*, 1996), although in the latter case the central pore-lining bundle of helices is held in place by an outer ring of other transmembrane elements. Thus, it seems likely that ion channels formed by M2 share a common structural architecture with a number of other channel proteins.

Several investigators have employed molecular modeling and simulation techniques to explore possible structures for ion channels formed by bundles of transmembrane helices (Kerr *et al.*, 1994, 1996; Montal, 1995). Such studies yield plausible candidate structures for ion channels which may be evaluated by further experimentation. Molecular modeling of channels formed by TM helix bundles is considerably aided if definitive experimental data are available on the number of helices per bundle and on the identity of the side chains of the helices associated with the ion permeation properties of a channel. As both of these conditions are met for M2 it is timely to use modeling and simulation techniques to explore possible molecular architectures for the TM domain of this integral membrane protein. In an earlier paper (Sansom and Kerr, 1993) a somewhat intuitive modeling procedure was used to generate a preliminary model of the M2 channel, in which the constituent α -helices formed extensive interactions only between their C-termini, resulting in a rather loose bundle structure. In the current investigation more automated, and objective, procedures have been used to develop models of the M2 channel in both its closed and open states. In these latter models the helix-to-helix interactions are more extensive than in the earlier model, resulting in a more compact helix tetrameric bundle in which the helices are tilted relative to the bilayer normal in agreement with recent solid state NMR data (Kovacs *et al.*, 1997). Simulations based on the more recent mod-

els are employed to formulate a hypothesis for the nature of the proton permeation pathway and of channel activation by low pH.

METHODS

General

Model building was performed using Xplor V3.1 (Brünger, 1992) with the CHARMM PARAM19 (Brooks *et al.*, 1983) parameter set. Only those H atoms attached to polar groups were represented explicitly; apolar groups were represented using extended carbon atoms. Visualization of models was carried out using Quanta V4.1 (Biosym/Molecular Simulations), and diagrams of structures were drawn using Quanta and Molscrip (Kraulis, 1991). MD simulations on the solvated models were performed using CHARMM (Brooks *et al.*, 1983) Version 23f3. Simulations were run on a DEC 2100 4/275. All other calculations were on Silicon Graphics R4000 workstations.

In vacuo modeling

Initial models of the M2 channel were generated by restrained molecular dynamics (MD) simulations, performed *in vacuo*, and by using a simulated annealing (Nilges and Brünger, 1991) protocol. The details of the method were as described in Kerr *et al.* (1994). Briefly, a C α template formed the starting point, defining the initial positions of the C α atoms of the M2 helices within a bundle, and thus embodying the assumptions discussed below. The remaining backbone and side-chain atoms were superimposed on the C α atoms of the corresponding residues. The C α atoms of the helices remained fixed throughout *Stage 1* of model generation. Annealing started at 1000 K, during which weights for covalent terms were gradually increased and a repulsive van der Waals potential was slowly introduced after an initial delay. Electrostatic terms were *not* included during *Stage 1*. *Stage 1* was repeated five times for each C α template, each resultant structure being subjected to five restrained MD runs (*Stage 2*), resulting in an ensemble of $5 \times 5 = 25$ final structures. During *Stage 2*, distance restraints (both intra- and interhelical—see below) were introduced, replacing the positional restraints on the positions of C α atoms used in *Stage 1*, and electrostatic interactions were gradually introduced into the potential energy function. All atoms were assigned partial charges as defined by the PARAM19 parameter set, and a distance-dependent dielectric ($\epsilon = r$) was used, with a switching function to smoothly truncate distant electrostatic interactions.

MD simulations of solvated pore models

Solvation of selected (see below) *in vacuo* models and extended MD simulations were carried out as described in Breed *et al.* (1996). Briefly, from each ensemble of 25

structures generated by *in vacuo* MD, that structure with the highest degree of rotational symmetry was refined by MD simulations in the presence of water molecules within and at the mouths of the pore. Pore models were solvated and MD simulations performed using protocols described previously (Breed *et al.*, 1996; Mitton and Sansom, 1996). Model pores were solvated in Quanta using preequilibrated boxes of water molecules. Water molecules were selected such that the central pore and the cap regions at either mouth of the pore were solvated, but such that no water molecules were present on the bilayer-exposed faces of the pores. The water model employed was a TIP3P three-site model (Jorgensen *et al.*, 1983) with partial charges $q_o = -0.834$ and $q_H = +0.417$.

The solvated model pore was energy minimized prior to refinement by MD simulation. During the MD simulations the following restraints were applied: (a) a cylindrical restraining potential on the waters (Breed *et al.*, 1996) to prevent evaporation from the mouths of the pore, (b) *intra*-helix restraints (between backbone NH and CO groups) (Breed *et al.*, 1996) to maintain the M2 transmembrane segments in an α -helical conformation, (c) *inter*-helix restraints (between the geometrical centers of adjacent helices in a bundle) to hold together the helix bundle (Kerr *et al.*, 1994, 1996), and (d) a bilayer potential, based on residue-by-residue hydrophobicities (Biggin and Sansom, 1996) to mimic the embedding of the helix bundle in a membrane. Trial simulations with different combinations of such restraints indicated that while they prevented the pore structure from drifting too far from the *in vacuo* model, they did not substantially alter the behavior of the water molecules either within or at the mouths of the pore, nor did they prevent a degree of repacking of the helices.

MD simulations employed a 1-fsec time step. The system was heated from 0 to 300 K in 6 psec (5 K, 0.1-psec steps) and equilibrated for 9 psec at 300 K by rescaling of atomic velocities every 0.1 psec. The production stage of the simulation was for 985 psec, giving a total simulation time of 1 nsec. During the production phase velocities were rescaled every 5 psec if the temperature strayed from within a window of 290 to 310 K. Trajectories were analyzed using coordinate sets saved every 1 psec during the production stage of the simulations. Non-bonded interactions (both electrostatic and van der Waals) between distant atoms were truncated using a shift function (Brooks *et al.*, 1983) with a cutoff of 13.0 Å, and a fixed dielectric of $\epsilon = 1$ was used for electrostatic interactions.

RESULTS

Generation of a $C\alpha$ template

At the outset of a modeling study it is important to state explicitly the assumptions underlying that study. The first of these concerns the sequence used for the

M2 TM helix. This was taken from the sequence of M2 of influenza A/chicken/FPV/Weybridge. The TM domain of M2 was defined using the program MEMSAT (Taylor *et al.*, 1994) to compare alternative topologies with one, two, or three TM helices per subunit. The highest scoring topology contained a single TM helix, with the sequence shown in Fig. 1A and with its N-terminus of the helix at the external face of the membrane. This assignment, based on sequence alone, is in agreement with experimental data on M2 (Lamb *et al.*, 1985), thus increasing confidence in the TM sequence prediction. Residues at positions 27, 30, 31, 34, 37, 38, and 41 have been identified as defining the face of the M2 helix which is critical for channel activity and/or amantadine sensitivity (Holsinger *et al.*, 1994).

As described above, an ensemble of 25 configurations of an isolated M2 helix was generated by *in vacuo* restrained MD simulations. In all models of M2 the N-terminus of the helix was blocked by an acetyl group and the C-terminus by an amide, in order to mimic the preceding and following peptide bonds within the intact protein. Five members of the ensemble of M2 helices are shown superimposed in Fig. 1B. Examination of these models reveals that the key residues (27, 30, 31, 34, 37, 38, and 41) lie on one face of the helix, defining a near-vertical band at an angle of ca. 5° to the helix axis.

Assumptions concerning the structure of the M2 pore are embodied in the $C\alpha$ template (Fig. 1C), which is an idealized model of the pore structure containing only the $C\alpha$ atoms used as a starting point for the *in vacuo* MD simulations. The pore is assumed to be formed by a bundle of four M2 helices. This is supported by experimental data (Holsinger and Lamb, 1991; Sugrue and Hay, 1991; Pinto *et al.*, 1997) which suggest that the M2 protein is tetrameric. The helix bundle is approximately parallel, i.e., the N-termini of the helices form one mouth of the pore and the C-termini form the other mouth. This is consistent with formation of disulfide bridges between cysteine residues of adjacent M2 monomers at sites just N-terminal to the TM helix. Within the bundle, the constituent helices are rotated about their long axes such that their channel-lining faces (defined above) are directed toward the center of the pore. Furthermore, the individual helices are tilted 5° relative to the pore (z) axis such that the overall geometry of the bundle is that of a left-handed supercoil. Such tilting of the helices ensures that all of the key residues (i.e., 27, 30, 31, 34, 37, 38, and 41) are directed toward the lumen of the pore. Thus the $C\alpha$ template embodies experimentally based assumptions concerning the nature of the M2 pore, and was used as the starting point for *in vacuo* molecular modelling.

Generation of initial models

The $C\alpha$ template was used to generate two ensembles, each of 25 structures, by *in vacuo* restrained MD simulations. Each ensemble started from the same $C\alpha$

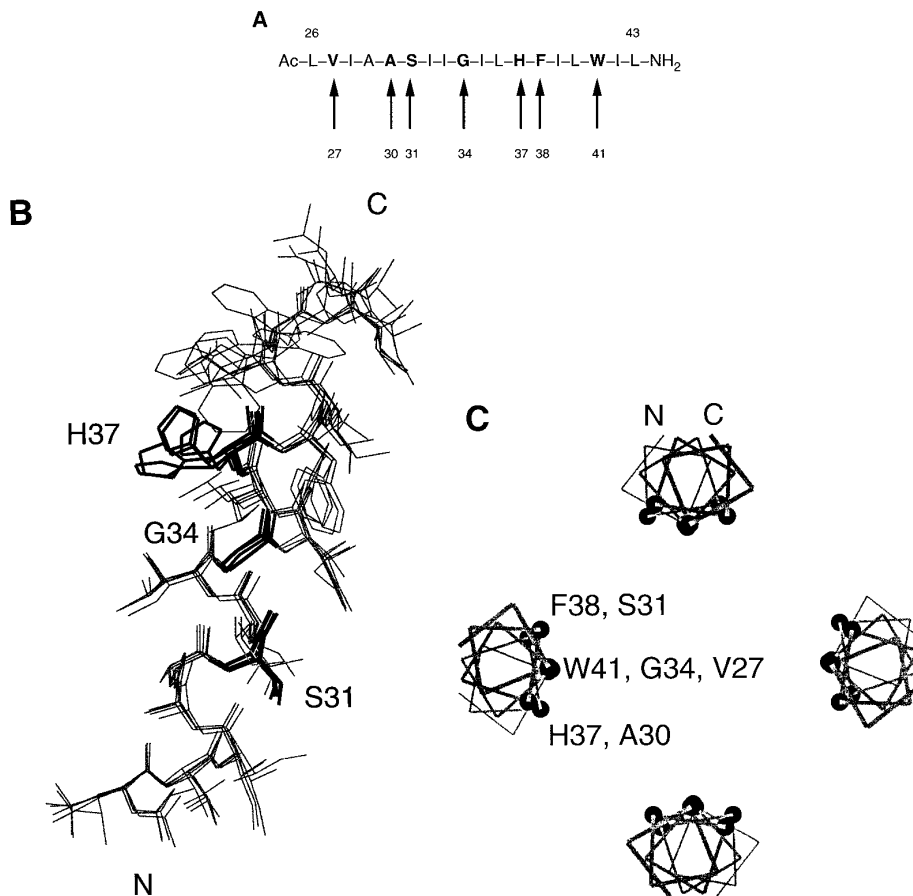


FIG. 1. (A) Sequence of the flu M2 transmembrane helix used in the modeling studies. Residues which have been suggested to correspond to the pore-lining face of the helix are indicated by arrows. (B) Models of an isolated flu M2 transmembrane helix. Five models of the helix, generated by *in vacuo* restrained MD simulations, are shown superimposed. Three key pore-lining residues (S31, G34, and H37) are shown using bold, black lines. The helix axis is tilted by 5°, so that the three pore-lining residues are arranged vertically. (C) C α template for the M2 helix bundles. The constituent helices of the bundle, which is viewed from the C-terminal mouth toward the N-terminal mouth, are tilted by 5° so as to form a left-handed supercoil. The C α 's of the pore-lining residues identified in A are shown as black spheres.

template, but they differed in the assumed protonation state of the histidine residue, H37. This residue has been suggested (Wang *et al.*, 1995) to govern activation of M2 channels by low pH. Accordingly two models were constructed: (a) a closed channel model, in which all four H37 residues were unprotonated, and (b) an open channel model in which all four H37 residues were protonated. Possible intermediate states, containing a mixture of protonated and unprotonated histidines, were not considered.

In vacuo MD simulations were run, using a standard protocol, to generate ensembles of structures for both the closed and the open models. Note that the starting C α template had the helices tilted to form an overall left-handed supercoil. The degree of helix tilt may be expressed in terms of the crossing angle (Ω ; see Chothia *et al.*, 1981) between adjacent helices. A positive crossing angle corresponds to a left-handed supercoil structure for the bundle as a whole. From the ensemble average of crossing angles (Table 1) it is evident that for both the closed and the open models the mean crossing angle increases relative to the C α template value of $\Omega = +8.8^\circ$.

This indicates that the extent of supercoiling of the helices increases during the course of the *in vacuo* simulations. The interhelix distance, set to an initial value of 13.2 Å in the C α template to ensure initial separation of the helices, converged to 10 Å in both ensembles, a value corresponding to close packing of adjacent helices.

A representative structure was selected from each ensemble, as the basis of further analysis and simulations. In general ion channels possess rotational symmetry about their central pore axis (Unwin, 1989; Oiki *et al.*, 1990). Thus the structure with the highest degree of rotational symmetry was selected from each ensemble. The two structures thus chosen are shown in Figs. 2A and 2B, in which the S31 and H37 side chains are indicated. From Table 1 it can be seen that in each selected structure, the degree of supercoiling is higher than that of the ensemble average, in that both the closed and the open model have helix crossing angles of Ω ca. +25°. Interhelix distances for both structures are compatible with close packing of adjacent helices. Thus, regardless of the charge state of the H37 residues it seems that an

TABLE 1
Packing of Helices

Model	Interhelix separation (Å)	Helix crossing angle (°)	Helix tilt ^a angle (°)
C α template	13.2	+8.8	6.2
Closed, <i>in vacuo</i> ensemble	10.0 (\pm 0.4)	+12.4 (\pm 7.9)	9.9 (\pm 4.9)
Closed, selected <i>in vacuo</i> structure	9.6 (\pm 0.2)	+25.9 (\pm 2.8)	15.6 (\pm 2.3)
Closed, solvated MD snapshots	9.8 (\pm 0.2)	+29.5 (\pm 5.4)	21.3 (\pm 2.7)
Open, <i>in vacuo</i> ensemble	10.0 (\pm 0.2)	+16.2 (\pm 8.2)	11.9 (\pm 5.8)
Open, selected <i>in vacuo</i> structure	10.0 (\pm 0.3)	+24.4 (\pm 1.9)	17.5 (\pm 3.0)
Open, solvated MD snapshots	10.1 (\pm 0.5)	+35.2 (\pm 4.2)	25.2 (\pm 4.2)

^a Relative to the bilayer normal.

M2 helix bundle adopts a stable left-handed supercoil structure. This corresponds to efficient ridges-in-grooves packing of the side chains (Chothia *et al.*, 1981) at the helix/helix interfaces and has previously been observed in simplified models of channels formed by hydrophobic helix bundles (Kerr *et al.*, 1994) and more recently in the crystal structure of a pentameric parallel bundle of α -helices which contains a central column of water molecules (Malashkevich *et al.*, 1996).

Examination of the closed and open models reveals a

striking difference. Although both models were generated starting from the same C α template, the helix orientation relative to the pore differs between them. Thus, in the closed model the H37 side chains are directed toward the center of the pore, while in the open model electrostatic repulsions between the protonated H37 side chains have resulted in a limited rotation of the helices such that the H37 side chains move away from the pore lumen to a more interfacial location. This helix rotation also means that in the open form of the channel, the S31 side chains point directly toward the lumen of the pore. In the closed model, the S31 side chains adopt a more interfacial location. This suggests a possible mechanism for gating of the channel, whereby protonation of H37 opens the pore. However, it should be remembered that these models are based on *in vacuo* simulations, and thus fail to take into account the interactions between the pore and water.

MD simulations with water

In order to refine the closed and open models of the M2 channel, extended MD simulations were performed with water molecules present within and at the mouths of their respective pores. Analysis of the behavior of the water molecules in these simulations provides insights into possible functional differences between the closed and the open models. A diagram of the simulation system (for the open model) is given in Fig. 3. In both cases the selected *in vacuo* model was solvated with about 150 waters in order to fill the pore with water and to provide caps of water at either mouth. During the MD simulation, an empirical bilayer potential was applied to the residues of the M2 helices to mimic the tendency of hydrophobic amino acids to embed themselves within a lipid bilayer (Biggin and Sansom, 1996). For each model the simulation was run for 1 nsec in order to allow a reasonable degree of relaxation of the corresponding *in vacuo* model in the presence of the solvent, and also to provide better statistical sampling for analysis of the dynamic properties of the water molecules.

Visual examination of the progress of the MD simulations suggested that major changes in helix packing did

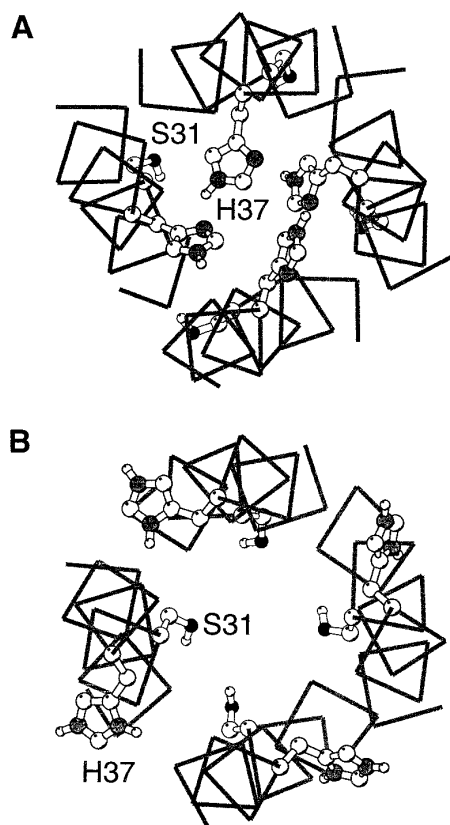


FIG. 2. (A) Structure of a closed pore model generated by *in vacuo* restrained MD. The most symmetrical member of the ensemble is shown. The bundle is viewed from the C-terminal mouth down the pore (z) axis. The side chains of S31 and H37 are shown in ball-and-stick format. (B) Corresponding diagram of an open pore model generated by *in vacuo* restrained MD.

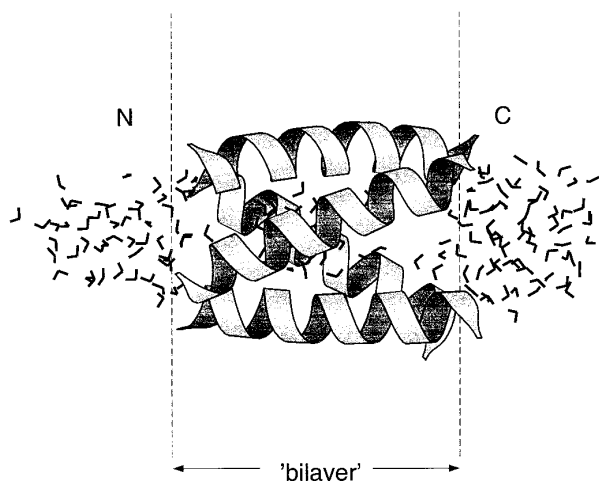


FIG. 3. MD simulations of solvated α -helix bundles. The open helix bundle is shown in ribbon format, along with the 151 water molecules within and at either mouth of the pore. The extent on z of the empirical bilayer potential is indicated by the two broken vertical lines.

not occur. For both models, the approximate fourfold rotational symmetry of the bundles was preserved throughout the simulations and, as can be seen from Table 1, the left-handed supercoiling of the M2 helices was retained. It should be noted that from the results of other, comparable, simulations (Bull and M. S. P. Sansom, unpublished results) we know that the interhelix distance restraints applied do not prevent changes in helix packing from occurring. Indeed, the degree of supercoiling in the M2 models did appear to increase to some extent over the 1-nsec duration of the simulations. Overall, we are confident that a left-handed supercoil is a stable packing arrangement of the M2 helices, as it is retained in both *in vacuo* and solvated simulations. One consequence of the supercoil structure is that the individual helices are tilted relative to the bilayer normal, by $21^\circ (\pm 3^\circ)$ for the closed model and by $25^\circ (\pm 4^\circ)$ for the open model (where the averages are over all four helices and the duration of the simulation). Such helix tilts are in agreement with recent solid-state NMR data (Kovacs *et al.*, 1997) on the orientation of synthetic peptide M2 helices reconstituted in phospholipid bilayers.

Snapshots of the MD simulation

Visual inspection of snapshots from the two solvated MD simulations suggests that the essential differences between the closed and the open channel models are preserved following solvation. In Fig. 4 two such snapshots, of the closed and of the open model, are shown in which the α -traces of the helices, the water molecules, and the H37 side chains are included. In the closed model (Fig. 4A) the unprotonated H37 side chains remain in the lumen of the pore, occluding it. Thus, in the closed model the water molecules extend into the lumen of the pore at the N-terminal mouth, forming a H-bonded network. This network of H-bonded waters is

interrupted by the ring of H37 side chains. There is also a cluster of waters at the C-terminal mouth of the pore. In the open model (Fig. 4B) the protonated H37 side chains are directed away from the lumen of the pore, although somewhat less so than in the corresponding *in vacuo* model. There is again an H-bonded network of water molecules extending from the N-terminal mouth of the pore toward the H37 ring. However, in the open model, because the histidine side chains do not point directly into the lumen, there are several water molecules which occupy the lumen of the pore in the vicinity of the H37 side chains, forming transient H-bonds to the water molecule network at the C-terminal mouth of the channel.

Thus, examination of a pair of single snapshots from the simulations suggests that in the closed model the H37 ring occludes the pore, preventing the formation of

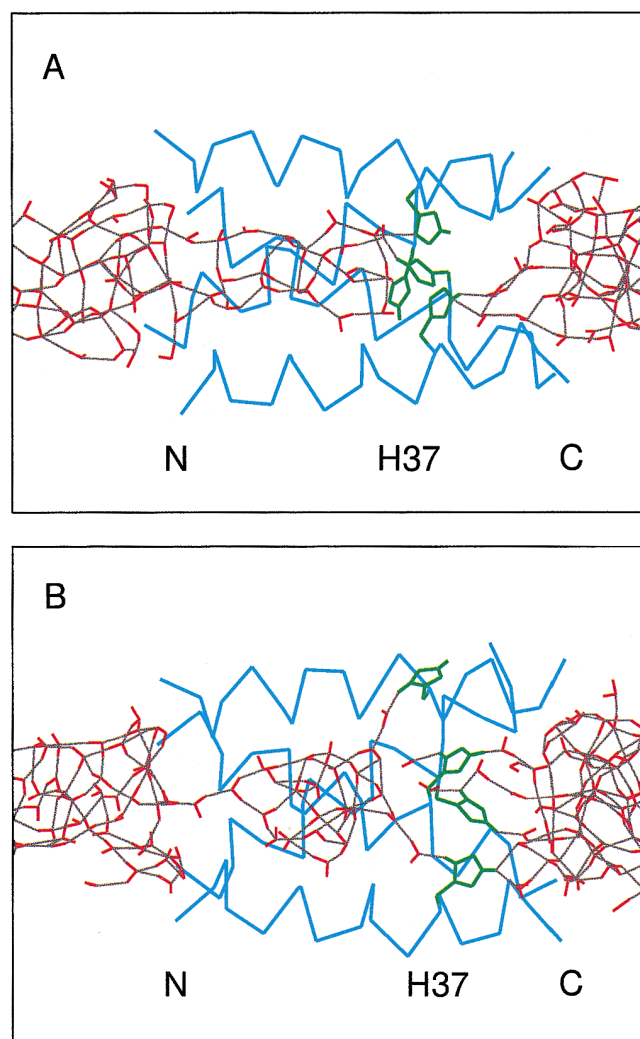


FIG. 4. (A) Snapshot of the closed pore + water MD simulation, at $t = 500$ psec. The α -helices are shown as blue α -traces, the water molecules as red bonds, the H37 side chains as green bonds, and the H-bonds formed by the waters as gray lines. The N-terminal mouth of the pore is on the left-hand side of the diagram. (B) Snapshot of the open pore + water MD simulation. Other details as for A.

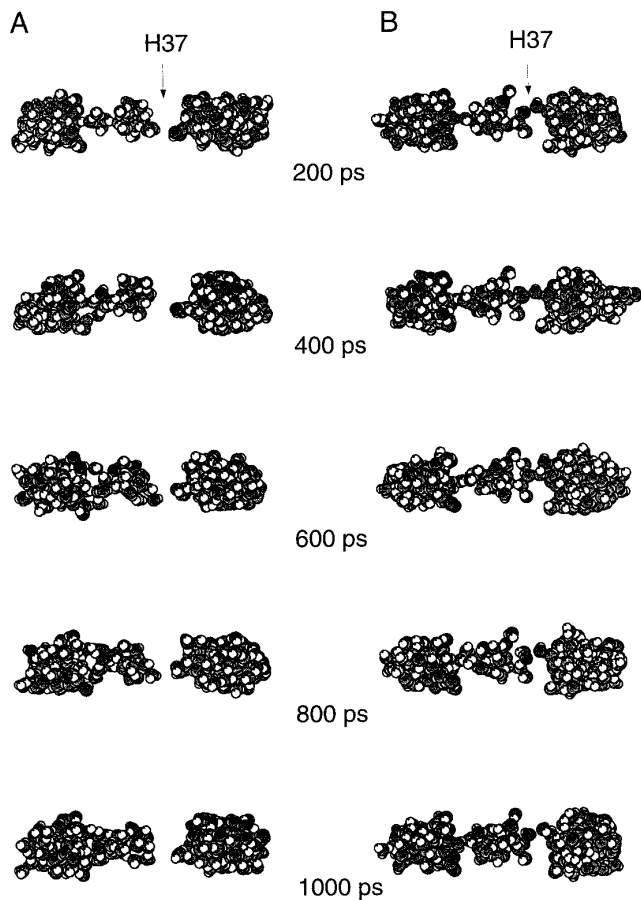


FIG. 5. Snapshots of the water molecules (shown in space-filling format) from the (A) closed and (B) open MD simulations. In each diagram the waters only are shown, viewed perpendicular to the pore (z) axis, with the left-hand side corresponding to the N-terminal mouth of the pore. For both systems, snapshots are shown for $t = 200, 400, 600, 800$, and 1000 psec.

a continuous column of water molecules, whereas in the open model there is a transient link between the water molecules on either side of the H37 ring. This is confirmed if one examines the positions of the water molecules alone from the two simulations throughout their 1-nsec duration. Thus, in Fig. 5 the water molecules only are shown, from the closed and open simulations, as two series of snapshots taken every 200-psec. In both cases there is a narrowing of the central column of waters in the vicinity of the H37 ring. In the closed simulation this narrowing generates a sustained break in the water column, whereas in the open simulation there is a fluctuating continuity of the water column across constriction of the pore formed by the H37 ring.

Water distribution within the pore

We have quantified differences in water distribution within the pores of the closed and open models. In Figs. 6A and 6B the numbers of waters in successive sections along the two pores, averaged across the duration of the two simulations, are compared. In both cases there are

significant numbers of waters in the N-terminal sections of the pore, although there is a dip in the number of waters in the vicinity of the N-terminal mouth of the open pore. In the open pore there is also a pronounced dip in the number of waters in the vicinity of the H37 ring. However, the average number of waters in this region does not fall to 0. In contrast, in the closed form of the pore there are *no* waters present in the vicinity of the H37 ring. This confirms that a continuous network of waters within the open pore is maintained throughout the simulation, once the system has relaxed from its initial *in vacuo* configuration.

A switch from closed to open

A third simulation was performed in order to evaluate more directly the proposal that protonation of the H37 side chains opens the M2 channel. This simulation

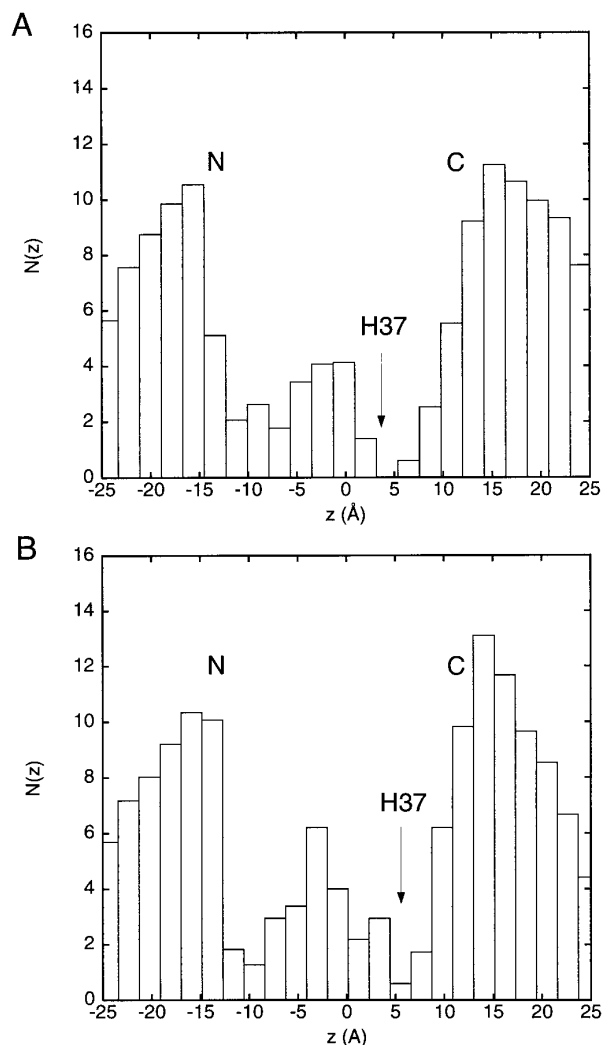


FIG. 6. Distribution of waters along the length of the pore. (A and B) The number of waters, $N(z)$, as a function of distance along the pore axis, z , for the closed and open MD simulations, respectively. In both cases the N-terminal mouth of the pore is at $z = -15$ Å and the C-terminal mouth is at $z = +12$ Å.

started with the structure taken from the end of the closed channel simulation, i.e., the 1000-psec structure of Fig. 5. This structure was modified by the addition of protons to the H37 side chains (using Quanta), just before the start of a further 550-psec MD simulation. The protocol for the simulation was the same as for the previous simulations of solvated M2 pores.

From visual inspection of the simulation it was evident that the H37 side chains, which initially occluded the channel, started to move away from the channel lumen during the heating and equilibration stages of the simulation. Once ca. 20 ps had elapsed, the change in structure of the channel was essentially complete. This removed the occlusion of the pore, indicating that the channel model had switched from a closed to an open conformation.

The effects of this switch in terms of the water molecules within the pore are shown in Fig. 7. In the initial structure there is a clear break in the column of water molecules in the vicinity of the H37 ring (see Fig. 5). By the time 150 psec have elapsed, water molecules have moved into this previously occluded region. The resultant continuity of the water column is maintained until the end of the 550-psec simulation. There is also a narrowing of the pore at the N-terminal mouth of the pore, in the vicinity of the ring of V27 side chains. This is also an echo of what is seen (Fig. 5) in the simulation starting from the *in vacuo*-generated open form of the channel.

DISCUSSION

Models of M2 channels

In an earlier, somewhat preliminary, model of the M2 channel (Sansom and Kerr, 1993) it was suggested that a wide-mouthed, conical pore was formed by radial tilting of the M2 helices away from the pore axis at their N-termini. In the current model this has been modified in favor of a more cylindrical pore in the current model for three reasons: (a) a conical model does not permit tight packing interactions of the M2 helices with one another, and so would be unlikely to correspond to a stable helix bundle; (b) a relatively wide-mouthed conical pore seems unlikely in the context of the observed H^+ selectivity of M2 channels (Chizhnikov *et al.*, 1996); and (c) the wide-mouthed, conical pore model was constructed on the basis of the assumption that amantadine acts as a simple open channel blocker (i.e., that amantadine binds within the pore). This latter assumption no longer seems to be supported by the experimental data. Indeed, data on the effects of mutations on amantadine block (Wang *et al.*, 1993; Holsinger *et al.*, 1994), on the differential effects of such mutations on M2 block by amantadine and by the spirene-containing compound BL-1743 (Tu *et al.*, 1996), and on the anti-viral activity of some rather bulky amantadine derivatives (Kolocouris *et al.*, 1996)

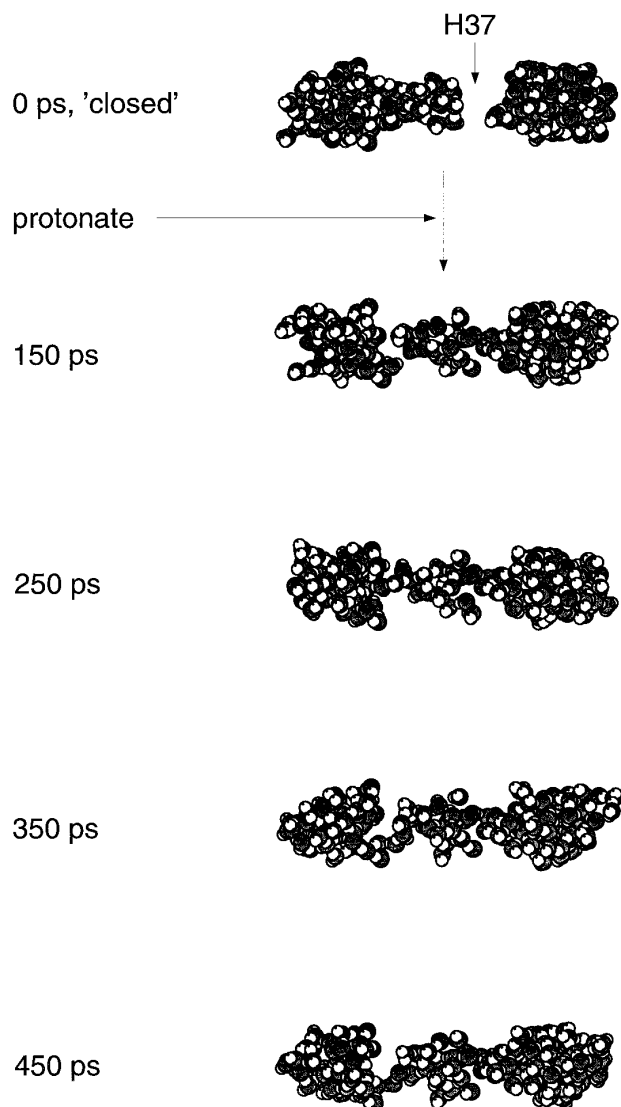


FIG. 7. Switch from a closed to an open channel. The simulation was started from the channel in its closed form, but the H37 side chains were protonated at $t = 0$. Snapshots (water molecules only, in space-filling format) are shown for the structures at $t = 150, 250, 350$, and 450 psec.

suggest a more complex mode of action of these drugs. One possibility is that they act in allosteric fashion (Pinto and Lamb, 1995), by preferential stabilization of the closed conformation of the M2 helix bundle.

We are confident that the current model represents a good approximation to the true M2 channel structure. In particular, we are encouraged by the agreement between the tilt of the helices relative to the bilayer normal in our model (20 to 25°) with the corresponding helix tilt (ca. 30°) observed in solid-state NMR studies of synthetic M2 helices in lipid bilayers (Kovacs *et al.*, 1997). Furthermore, the relatively narrow pore present in the current model, compared with that in Sansom and Kerr (1993), is more consistent with a H^+ selective pore. Finally, the left-handed supercoil structure of the bundle enables optimal packing of the side chains of adjacent helices.

A model for permeation and gating

The simulations presented in this paper provide a plausible model for how the influenza A protein forms H⁺-permeable pores, and how such pores may be activated by low pH. We now review the model, the support which it receives from available experimental evidence, and its relationship to models of other channels which enable H⁺ permeation.

It is proposed that TM helices of four M2 subunits form a narrow, water-filled pore. The water within this pore is immobile relative to bulk water, and in the open form of the channel a fluctuating H-bonded network is formed along the entire length of the pore. Thus, H⁺ permeability may arise by protons hopping from water to water, the waters being held in place by the channel. That is, the immobilized water within the channel forms a proton wire (Deamer, 1996). If this is so, then to a first approximation, the mechanism of H⁺ transfer is somewhat independent of the exact nature of the side chains lining the pore. In the open state of the channel the pore is lined by residues V27, S31, G34, F38, and W41. A comparison of M2 sequences suggests that the residues in the N-terminal half of the TM helix are somewhat less strictly conserved than those in the C-terminal half. For example, V27, which guards the N-terminal mouth of the pore, may be replaced by a polar threonine side chain. Furthermore, experimental mutation of V27 to a more polar (V27S or V27T) or smaller (V27A) side chain (Holsinger *et al.*, 1994) results in an approximately threefold increase in channel activity, although it is not known whether this reflects an increase in single channel conductance. Similarly, S31 is replaced by an asparagine in some M2 sequences, again a polar yet uncharged side chain. G34, which allows the existence of a more extended water-filled pocket in the center of the pore, is generally conserved. However, the experimental mutation G34E results in an increase in channel activity (Holsinger *et al.*, 1994). In the C-terminal half of the TM helix, F38 is replaced by a leucine in some M2 sequences. W41, which is responsible for the C-terminal constriction of the pore even when in its open form, is strictly conserved. Furthermore, experimental mutation of residue 41 (W41A) leads to a complete loss of channel activity (Holsinger *et al.*, 1994). This suggests that the constriction of the pore at its C-terminus by the ring of W41 side chains is essential for its structure and/or function. As noted above, the W41-induced constriction of the pore is such that only a single water molecule may be accommodated. Perhaps this is essential for M2 channel function.

Comparison of the open and closed forms of the model suggests that protonation/deprotonation of H37 may control the gating of the channel. It is proposed that when unprotonated (i.e., uncharged) the H37 side chains are oriented inward and thus occlude the pore. A simulation starting from this closed state in which the H37 side

chain were protonated resulted in a structural switch which reopened the channel. Significantly, replacement of H37 by either a glycine (H37G) or a glutamate (H37E) results in channels which are no longer activated by low pH (Wang *et al.*, 1995). In the context of the current model, the H37G mutant would be expected to allow a continuous column of water to be formed even when the helix bundle was in its closed conformation, whereas the introduction of a glutamate residue in H37E might be expected to lock the bundle in its open conformation, via electrostatic repulsions between the glutamate side chains.

Examination of the relationship of the current model to models of other H⁺-permeable channels is informative. Simulation studies of H⁺ conductance by the simple antibiotic peptide gramicidin A (Pomes and Roux, 1996; Sagnella *et al.*, 1996) stress the role of H⁺ hopping along a wire of immobilized water molecules. Selective H⁺ permeability is observed in channels formed by a *de novo* designed amphipathic α -helical peptide synthesized and characterized by DeGrado and colleagues (Lear *et al.*, 1988). Significantly, the H⁺-permeable pores formed by the latter peptide have been shown to be consistent with formation of tetrameric α -helix bundles (Åkerfeldt *et al.*, 1992). Recent MD simulations of such tetrameric α -helix bundles also support the formation of a wire of immobilized water molecules (Mitton and Sansom, 1996). However, it should be noted that DeCoursey and Cherny (1997) have suggested that the voltage-activated H⁺ channel of rat alveolar epithelium does *not* behave like a water-filled pore. It therefore seems that there may be a diversity of mechanisms by which a TM protein may confer a H⁺ conductance on a membrane.

Extending the simulations

The current simulations are, of course, at best an approximation of the true behavior of the M2 channel. The major approximations are the absence from the MD simulations of an explicit representation of the lipid bilayer and the absence from the channel model of the extramembraneous N- and C-terminal segments of the protein. The absent bilayer was represented in the simulations by an empirical side chain hydrophobicity potential which has been used in a number of other simulations of membrane proteins (Edholm and Jahnig, 1988; Jahnig and Edholm, 1992; Milik and Skolnick, 1993, 1995; Biggin and Sansom, 1996). The absent protein segments, particularly the N-terminal disulfide bridges, may be expected to further stabilize the TM helix bundle. However, the demonstration of amantadine-sensitive channels formed by synthetic peptides (Duff and Ashley, 1992) suggests that the channel properties of M2 reside primarily in its TM helices. A further approximation is the use of the relatively TIP3P water model, although this has been used in numerous simulations of protein/water interactions (Roux and Karplus, 1991; Knapp and Muegge, 1993; Komeiji *et al.*, 1993).

Further studies are needed to refine both the M2 model and the simulation procedure. To improve the model it will be necessary to include at least the disulfide bridge-forming region of the N-terminal segment of M2. The resultant model may then be embedded in an explicit bilayer or surrounded by an annulus of lipid molecules (Woolf and Roux, 1996). Simulations using such a system might employ a model of water (PM6) which has been used to simulate proton movements within the gramicidin pore (Pomes and Roux, 1996). The permeability of the open channel model to monovalent metal cations (Shimbo *et al.*, 1996) could also be explored by simulations.

Finally, the methods used in this paper may be applicable to other simple ion channel proteins from viruses. These include the NB protein from influenza virus (Sunstrom *et al.*, 1996) and the Vpu protein from HIV-1 (Ewart *et al.*, 1996; Schubert *et al.*, 1996), both of which have been shown to form ion channels in planar bilayers and in *Escherichia coli* cell membranes. Preliminary simulation results (Grice *et al.*, 1997) suggest that model building and simulation will provide valuable insights into possible ion permeation mechanisms provided by these less well characterized viral proteins (Lamb and Pinto, 1997).

ACKNOWLEDGMENTS

This work was supported by a grant from the Wellcome Trust. Our thanks to the Oxford Centre for Molecular Science for the use of computational facilities.

REFERENCES

- Akerfeldt, K. S., Kim, R. M., Camac, D., Groves, J. T., Lear, J. D., and DeGrado, W. F. (1992). Tetraphilin: A four-helix proton channel built on a tetraphenylporphyrin framework. *J. Am. Chem. Soc.* **114**, 9656–9657.
- Arkin, I. T., Rothman, M., Ludlam, C. F. C., Aimoto, S., Engelman, D. M., Rothschild, K. J., and Smith, S. O. (1995). Structural model of the phospholamban ion channel complex in phospholipid membranes. *J. Mol. Biol.* **248**, 824–834.
- Biggin, P. C., and Sansom, M. S. P. (1996). Simulation of voltage-dependent interactions of α -helical peptides with lipid bilayers. *Biophys. Chem.* **60**, 99–110.
- Breed, J., Sankaramakrishnan, R., Kerr, I. D., and Sansom, M. S. P. (1996). Molecular dynamics simulations of water within models of transbilayer pores. *Biophys. J.* **70**, 1643–1661.
- Brooks, B. R., Brucoleri, R. E., Olafson, B. D., States, D. J., Swaminathan, S., and Karplus, M. (1983). CHARMM: A program for macromolecular energy, minimisation, and dynamics calculations. *J. Comp. Chem.* **4**, 187–217.
- Brünger, A. T. (1992). "X-PLOR Version 3.1: A System for X-Ray Crystallography and NMR." Yale Univ. Press, New Haven, CT.
- Chizhnikov, I. V., Geraghty, F. M., Ogden, D. C., Hayhurst, A., Antoniou, M., and Hay, A. J. (1996). Selective proton permeability and pH regulation of the influenza virus M2 channel expressed in mouse erythro-leukaemia cells. *J. Physiol.* **494**, 329–336.
- Chothia, C., Levitt, M., and Richardson, D. (1981). Helix to helix packing in proteins. *J. Mol. Biol.* **145**, 215–250.
- Ciampor, F., Bayley, P. M., Nermut, M. V., Hirst, E. M. A., Sugrue, R. J., and Hay, A. J. (1992). Evidence that the amantadine-induced, M2-mediated conversion of influenza-A virus haemagglutinin to the low pH conformation occurs in an acidic *trans*-Golgi compartment. *Virology* **188**, 14–24.
- Deamer, D. W. (1996). Visualizing proton conductance in the gramicidin channel. *Biophys. J.* **71**, 5.
- DeCoursey, T. E., and Cherny, V. V. (1997). Deuterium isotope effects on permeation and gating of proton channels in rat alveolar epithelium. *J. Gen. Physiol.* **109**, 415–434.
- Duff, K. C., and Ashley, R. H. (1992). The transmembrane domain of influenza A M2 protein forms amantadine-sensitive proton channels in planar lipid bilayers. *Virology* **190**, 485–489.
- Duff, K. C., Kelly, S. M., Price, N. C., and Bradshaw, J. P. (1992). The secondary structure of influenza A M2 transmembrane domain. *FEBS Lett.* **311**, 256–258.
- Edholm, O., and Jähnig, F. (1988). The structure of a membrane-spanning polypeptide studied by molecular dynamics. *Biophys. Chem.* **30**, 279–292.
- Ewart, G. D., Sutherland, T., Gage, P. W., and Cox, G. B. (1996). The Vpu protein of human immunodeficiency virus type 1 forms cation-selective ion channels. *J. Virol.* **70**, 7108–7115.
- Grice, A., Kerr, I. D., and Sansom, M. S. P. (1997). Ion channels formed by HIV-1 Vpu: A modelling and simulation study. *FEBS Lett.* **405**, 299–304.
- Hay, A. J., Wolstenholme, A. J., Skehel, J. J., and Smith, M. H. (1985). The molecular basis of the specific anti-influenza action of amantadine. *EMBO J.* **4**, 3021–3024.
- Helenius, A. (1992). Unpacking the incoming influenza virus. *Cell* **69**, 577–578.
- Holsinger, L. J., and Lamb, R. A. (1991). Influenza virus M₂ integral membrane protein is a homotetramer stabilized by formation of disulphide bonds. *Virology* **183**, 32–43.
- Holsinger, L. J., Nichani, D., Pinto, L. H., and Lamb, R. A. (1994). Influenza A virus M₂ ion channel protein: A structure–function analysis. *J. Virol.* **68**, 1551–1563.
- Jähnig, F., and Edholm, O. (1992). Modeling of the structure of bacteriorhodopsin: A molecular dynamics study. *J. Mol. Biol.* **226**, 837–850.
- Jorgensen, W. L., Chandrasekhar, J., Madura, J. D., Impey, R. W., and Klein, M. L. (1983). Comparison of simple potential functions for simulating liquid water. *J. Chem. Phys.* **79**, 926–935.
- Kerr, I. D., Doak, D. G., Sankaramakrishnan, R., Breed, J., and Sansom, M. S. P. (1996). Molecular modelling of staphylococcal δ -toxin ion channels by restrained molecular dynamics. *Protein Eng.* **9**, 161–171.
- Kerr, I. D., Sankaramakrishnan, R., Smart, O. S., and Sansom, M. S. P. (1994). Parallel helix bundles and ion channels: Molecular modelling via simulated annealing and restrained molecular dynamics. *Biophys. J.* **67**, 1501–1515.
- Knapp, E. W., and Muegge, I. (1993). Heterogeneous diffusion of water at protein surfaces: Application to BPTI. *J. Phys. Chem.* **97**, 11339–11343.
- Kolocouris, N., Kolocouris, A., Foscolos, G. B., Fytas, G., Neyts, J., Paldalko, E., Balzarini, J., Snoeck, R., Andrei, G., and De Clercq, E. (1996). Synthesis and antiviral activity evaluation of some new aminoadamantane derivatives. *J. Med. Chem.* **39**, 3307–3318.
- Komeiji, Y., Uebayasi, M., Someya, J., and Yamato, I. (1993). A molecular dynamics study of solvent behavior around a protein. *Proteins Struct. Funct. Genet.* **16**, 268–277.
- Kovacs, F. A., Brennen, M. T., Quine, J., and Cross, T. A. (1997). Structural characterization of the M2 transmembrane peptide backbone using solid state NMR. *Biophys. J.* **72**, A399.
- Kraulis, P. J. (1991). MOLSCRIPT: A program to produce both detailed and schematic plots of protein structures. *J. Appl. Crystallogr.* **24**, 946–950.
- Kurtz, S., Luo, G., Hahnenberger, K. M., Brooks, C., Gecha, O., Ingalls, K., Numata, K. I., and Krystal, M. (1995). Growth impairment resulting from expression of influenza virus M2 protein in *Saccharomyces cerevisiae*: Identification of a novel inhibitor of influenza virus. *Antimicrob. Agents Chemother.* **39**, 2204–2209.
- Lamb, R. A., and Pinto, L. H. (1997). Do Vpu and Vpr of human immuno-

- deficiency virus type 1 and NB of influenza B virus have ion channel activities in the viral life cycle? *Virology* **229**, 1–24.
- Lamb, R. A., Zebedee, S. L., and Richardson, C. D. (1985). Influenza virus M₂ protein is an integral membrane protein expressed on the infected-cell surface. *Cell* **40**, 627–633.
- Lear, J. D., Wasserman, Z. R., and DeGrado, W. F. (1988). Synthetic amphiphilic peptide models for protein ion channels. *Science* **240**, 1177–1181.
- Malashkevich, V. N., Kammerer, R. A., Efimov, V. P., Schulthess, T., and Engel, J. (1996). The crystal structure of a five-stranded coiled coil in COMP: A prototype ion channel? *Science* **274**, 761–765.
- Milik, M., and Skolnick, J. (1993). Insertion of peptide chains into lipid membranes: An off-lattice Monte Carlo dynamics model. *Proteins Struct. Funct. Genet.* **15**, 10–25.
- Milik, M., and Skolnick, J. (1995). A Monte Carlo model of fd and Pf1 coat proteins in lipid membranes. *Biophys. J.* **69**, 1382–1386.
- Mitton, P., and Sansom, M. S. P. (1996). Molecular dynamics simulations of ion channels formed by bundles of amphipathic α -helical peptides. *Eur. Biophys. J.* **25**, 139–150.
- Montal, M. (1995). Design of molecular function: Channels of communication. *Annu. Rev. Biophys. Biomol. Struct.* **24**, 31–57.
- Nilges, M., and Brunger, A. T. (1991). Automated modelling of coiled coils: Application to the GCN4 dimerization region. *Protein Eng.* **4**, 649–659.
- Oiki, S., Madison, V., and Montal, M. (1990). Bundles of amphipathic transmembrane α -helices as a structural motif for ion conducting channel proteins: Studies on sodium channels and acetylcholine receptors. *Proteins Struct. Funct. Genet.* **8**, 226–236.
- Panayotov, P. P., and Schlesinger, R. W. (1992). Oligomeric organization and strain-specific proteolytic modification of the virion M2 protein of influenza A H1N1 viruses. *Virology* **186**, 352–355.
- Pinto, L. H., Holsinger, L. J., and Lamb, R. A. (1992). Influenza virus M₂ protein has ion channel activity. *Cell* **69**, 517–528.
- Pinto, L. H., and Lamb, R. A. (1995). Understanding the mechanism of action of the anti-influenza virus drug amantadine. *Trends Microbiol.* **3**, 271.
- Pinto, L. H., Tu, Q., Sakeguchi, T., Gandhi, C., and Lamb, R. A. (1997). The active oligomeric state of the influenza virus M2 ion channel is a tetramer. *Biophys. J.* **72**, A109.
- Pomes, R., and Roux, B. (1996). Structure and dynamics of a proton wire: A theoretical study of H⁺ translocation along the single-file water chain in the gramicidin A channel. *Biophys. J.* **71**, 19–39.
- Roux, B., and Karplus, M. (1991). Ion transport in a model gramicidin channel: Structure and thermodynamics. *Biophys. J.* **59**, 961–981.
- Sagnella, D. E., Laason, K., and Klein, M. L. (1996). Ab initio molecular dynamics study of proton transfer in a polyglycine analog of the ion channel gramicidin. *Biophys. J.* **71**, 1172–1178.
- Sankaramakrishnan, R., Adcock, C., and Sansom, M. S. P. (1996). The pore domain of the nicotinic acetylcholine receptor: Molecular modelling and electrostatics. *Biophys. J.* **71**, 1659–1671.
- Sansom, M. S. P. (1991). The biophysics of peptide models of ion channels. *Prog. Biophys. Mol. Biol.* **55**, 139–236.
- Sansom, M. S. P. (1993). Structure and function of channel-forming peptides. *Q. Rev. Biophys.* **26**, 365–421.
- Sansom, M. S. P., and Kerr, I. D. (1993). Influenza virus M2 protein: A molecular modelling study of the ion channel. *Protein Eng.* **6**, 65–74.
- Schroeder, C., Ford, C. M., Wharton, S. A., and Hay, A. J. (1994). Functional reconstitution in lipid vesicles of influenza virus M2 protein expressed by baculovirus: Evidence for proton transfer activity. *J. Gen. Virol.* **75**, 3477–3484.
- Schubert, U., Ferrer-Montiel, A. V., Oblatt-Montal, M., Henklein, P., Strebel, K., and Montal, M. (1996). Identification of an ion channel activity of the Vpu transmembrane domain and its involvement in the regulation of virus release from HIV-1-infected cells. *FEBS Lett.* **398**, 12–18.
- Shimbo, K., Brassard, D. L., Lamb, R. A., and Pinto, L. H. (1996). Selectivity and activation of the M₂ ion-channel of influenza-virus. *Biophys. J.* **70**, 1335–1346.
- Sugrue, R. J., and Hay, A. J. (1991). Structural characteristics of the M2 protein of influenza A viruses: Evidence that it forms a tetrameric channel. *Virology* **180**, 617–624.
- Sunstrom, N. A., Prekumar, L. S., Prekumar, A., Ewart, G., Cox, G. B., and Gage, P. W. (1996). Ion channels formed by NB, an influenza B virus protein. *J. Membr. Biol.* **150**, 127–132.
- Taylor, W. R., Jones, D. T., and Green, N. M. (1994). A method for α -helical integral membrane protein fold prediction. *Proteins Struct. Funct. Genet.* **18**, 281–294.
- Tosteson, M. T., Pinto, L. H., Holsinger, L. J., and Lamb, R. A. (1994). Reconstitution of the influenza virus M₂ ion channel in lipid bilayers. *J. Membr. Biol.* **142**, 117–126.
- Tu, Q., Pinto, L. H., Luo, G., Shaughnessy, M. A., Mullaney, D., Kurtz, S., Krystal, M., and Lamb, R. A. (1996). Characterization of inhibition of M₂ ion channel activity by BL-1743, an inhibitor of influenza A virus. *J. Virol.* **70**, 4246–4252.
- Unwin, N. (1989). The structure of ion channels in membranes of excitable cells. *Neuron* **3**, 665–676.
- Unwin, N. (1995). Acetylcholine receptor channel imaged in the open state. *Nature* **373**, 37–43.
- Wang, C., Lamb, R. A., and Pinto, L. H. (1994). Direct measurement of the influenza A virus M₂ protein ion channel activity in mammalian cells. *Virology* **205**, 133–140.
- Wang, C., Lamb, R. A., and Pinto, L. H. (1995). Activation of the M2 ion channel of influenza virus: A role for the transmembrane domain histidine residue. *Biophys. J.* **69**, 1363–1371.
- Wang, C., Takeuchi, K., Pinto, L. H., and Lamb, R. A. (1993). Ion channel activity of influenza A virus M₂ protein: Characterization of the amantadine block. *J. Virol.* **67**, 5585–5594.
- Woolf, T. B., and Roux, B. (1996). Structure, energetics, and dynamics of lipid-protein interactions—A molecular-dynamics study of the gramicidin-A channel in a DMPC bilayer. *Proteins Struct. Funct. Genet.* **24**, 92–114.